Forced Convective Heat Transfer in Al_2O_3-air Nanoaerosol

Maulin D. Trivedi, Craig T. Johansen

University of Calgary, Calgary, Alberta, T2N 1N4, Canada

Hotwire experiments were performed to assess the effects of suspended 100 nm diameter aluminum oxide (Al_2O_3) nanoparticles in air on the rate of convective heat transfer. The particle mass loading ($0.01\% < S_L < 0.1\%$) was varied over a range of Reynolds numbers ($1420 < Re < 10{,}310$), while monitoring the global Nusselt number. The results indicate up to a 45% increase in the Nusselt number over the baseline air case for a particle mass loading of 0.1% at a Reynolds number of 7,500. The enhancement to heat transfer is an order of magnitude larger compared to results from related heat transfer experiments reported in the literature that used micron-sized aerosols at similar particle mass loadings. Potential application of the dispersion of nanoparticles into the intake air of a high-speed propulsion system is discussed.

Nomenclature

ρ	Density, kg/m^3
m	Mass, kg
$\dot{m}$	Mass Flow Rate, kg/s
V	Volume, m^3
C	Heat Capacity, kJ/kgK
Φ	Particle Volumetric Loading
μ	Viscosity, Ns/m^2
k	Thermal Conductivity, W/mK
n	Empirical Shape Factor
Re	Reynolds Number
U	Fluid Velocity, m/s
D	Pipe Diameter, m
Pr	Prandtl Number
Nu	Nusselt Number
Q	Internal Energy, W
Q	Internal Energy, W
S_L	Particle Mass Loading
h	Convective Heat Transfer Coefficient, W/m^{2}K
A	Cross Sectional Area of Hot-wire, m^2

Subscript

p	Particle
f	Base Fluid
eff	Effective
s	Hot-wire Surface
d	Down-stream of Hot-wire
u	Up-stream of Hot-wire
in	Free-stream

I. Introduction

The addition of solid nanoparticles to a fluid to improve bulk flow properties is an active area of research. Nanoparticles are defined as particles with diameters between 1 nm and 100 nm; in addition, they exhibit properties not found in bulk samples of the same material.[1] Nanoparticles are commonly suspended in fluids referred to as nanofluids (when using liquid phase fluid) or nanoaerosols (when using gaseous phase fluid) to enhance heat transfer characteristics such as thermal conductivity and convective heat transfer coefficient.[1] Such characteristics make them ideal for a wide range of engineering applications. According to a case study by Routbort et al. (2012), replacement of heating and cooling water with nanofluids could result in energy conservation of 10-30 trillion Btu/year in the United States.[2] The result would be a reduction in emissions i.e. 5.6 million metric tons of carbon dioxide, 8600 metric tons of nitrogen oxide and 21,000 metric tons of sulfur dioxide. Compared to meso- or micro-particles, nanoparticles provide higher heat transfer and stability while reducing clogging, erosion and pumping power.[3] For nanoaerosols, Schluderberg et al. studied the use of graphite dust suspension in air to enhance the heat transfer of a nuclear reactant coolant.[4]

Nanoparticles have also gained interest for aerospace applications. In a work by Goroshin et al. (2001), metallic nanopowders were evaluated as alternative fuels in hypersonic ramjets.[5] Metallic fuels are desirable as they have high energy contents per unit volume and per unit mass. Boron, for example, has higher energy content per unit mass than typical hydrocarbon fuels and higher energy content per unit volume than both hydrogen (uncompressed) and hydrocarbon fuels. Metallic nanoparticles have excellent storage qualities and do not produce carbon dioxide when combusted. It has been found experimentally that nanoparticles typically have a lower melting point, ignite at lower temperatures, and have a higher burning rate than larger scale particles.[6] Enhancing heat transfer for high-speed propulsion systems can have a large impact on engine performance. For example, precooled turbojects, which actively cool the compressed intake air, can operate at high specific impulses at high Mach numbers, while still providing significant thrust at low Mach numbers.[7] Reaction Engines Limited is developing a precooled turbojet concept, which relies on an elaborate tube in cross-flow heat exchanger to remove heat from the flow.[8,9] Space Engine Systems Inc. is developing a similar concept (DASS Engine), but aims to reduce the size of the heat exchanger by using the dispersion of metallic nanoparticles to enhance the rate of convective heat transfer. It is clear that the ability to understand and predict the level of heat transfer enhancement is key for the development of these engine concepts.

The majority of experimental and theoretical research work related to heat transfer enhancement is based on particle-liquid mixtures.[10–23] Analytical relations based on the principle of a two-component mixture are used to predict density, heat capacity, viscosity and thermal conductivity of nanofluids. Experiments conducted by Pak and Cho (1998) and Ho et al. (2010) using Al_2O_3-water nanofluid validate the relation for density.[24,25] Similarly, predicted heat capacity of nanofluids compares very well to experimental data from Zhou and Ni (2008) for Al_2O_3-water nanofluids with volume fraction 0-21.7%.[26] Despite studies from many researchers, there are no inviolable models available to predict viscosity and thermal conductivity of nanofluids.[27] Effective viscosity of Al_2O_3-water nanofluid can be predicted from available models for low particle concentration ($\Phi_p \leq 2\%$). However, significant underestimation is observed when compared to experimental data from Khanafer et al. (2011), Maiga et al. (2005), Buongiorno (2006), and Nguyen et al (2007).[27–30] Similarly, an empirical correlation is required to accurately predict effective thermal conductivity. The Hamilton-Crosser model can be used for low concentrations ($\Phi_p \leq 2\%$).[31] Available models and experimental data show large discrepancies in results even for same base fluid and nanoparticle size. Choi et al. (1995) predicted thermal conductivity of CuO-water nanofluid using the Hamilton-Crosser relation. It was found that thermal conductivity increased by 150% and 350% for volume fractions of 5% and 20%, respectively when using constant nanoparticle sphericity of 0.3. This enhancement was verified by experimental work of Xuan et al. (2000) using transient hot wire method and CuO-water nanofluid.

Factors such as flow pattern, Reynolds number, Prandtl number, temperature, volume fraction, size and shape of particles along with effective thermal conductivity and heat capacity also affect the heat transfer coefficient of nanofluids.[32] Experiments conducted by Heris et al. (2006) using Al_2O_3-water nanofluids show as high as 40% increase in the heat transfer coefficient and approximately 15% increase in the thermal conductivity.[33] Similar results were obtained from experiments conducted by Xuan and Li (2002) using Cu-water nanofluids. Their results show approximately 36% increase in the heat transfer coefficient for 2% volume concentration. Other researchers have reported comparable heat transfer enhancement using nanofluids.[15,19,23,34–38] On the contrary, results from Pak and Cho (1998) demonstrate 12% decrease in convective heat transfer coefficient for 3% volume concentration of Al_2O_3-water despite an increase in Nusselt num-

ber. Contradictory evidence has made it difficult to distinguish mechanisms for heat transfer enhancement resulting in the lack of accurate theoretical model.

Murray (1994) and Williams (2015) give an excellent overview of particle-gas suspensions.[39,40] Murray argues that the main mechanisms for heat transfer enhancement are (1) increased thermal capacity of the suspensions; (2) conduction between impacting particles; (3) thermal energy transport by rebounding particles; and (4) changes in the boundary-layer characteristics and turbulent structure of the gas flow. Murray suggests a multiplicative relationship between effects of increased thermal capacity, effective flow Reynolds number and turbulence modification by particles to predict an overall enhancement in microparticles-gas suspension flows. He also explains that for smaller particles that the primary enhancement mechanism is attributed to changes in the thermal capacity (1) of the mixture. Solid particles, with a high density, increase the overall volumetric heat capacity despite having similar specific heats (c_p) as the carrier gas. Williams argues that the effects of thermopheresis, Brownian diffusion, agglomeration, thermal conductivity increase, and radiation are small for typical nanoaerosols at moderate temperatures.[40]

Murray conducted experiments to measure heat transfer for solid-gas suspension using a staggered tube array.[41] The experiment used glass beads with diameter of 46, 58 and 127 μm with density of 2700 kg/m^3, specific heat of 910 J/kgK, and thermal conductivity of 1.4 W/mK. His results show a positive correlation between Nusselt number and mass loading of solid particles at constant Reynolds number. As predicted, an increase in Nusselt number was observed as the particle size decreased. At constant particle size, Nusselt number ratio decreased with an increase in flow Reynolds number due to shorter particle residence time.

Although micro-sized particle suspensions show enhanced rates of heat transfer, they have major disadvantages for industrial applications due to settling, eroding, clogging and higher pressure loss for flow. However, modern manufacturing technology has allowed for production of nanometer sized particles. Using nanoparticles compared to micro-particles allows higher heat conduction while reducing previously mentioned issues. They also provide large surface area to volume ratio, less particle momentum and high mobility.[3]

The vast majority of research in this area is focused on nanoparticles suspended in liquids and micron-sized particles suspended in gases. To the authors' knowledge, experimental investigation regarding heat transfer enhancement in nanoaerosols has been very limited. The present work reports on early results from a heat transfer experiment using 100 nm Al2O3 -air nanoaerosol.

II. Experimental Set-Up

A forced convection experimental apparatus was constructed to disperse a dilute amount of nanoparticles into an air flow. The nanoaerosol was flowed in a 10.16 mm diameter tube past a heated Nichrome wire (hot-wire) that was oriented in a cross-flow configuration with respect to the flow. Heat transfer from the hot-wire resulted in an increase in mixture temperature. Temperature measurements both upstream and downstream of the heated wire were used to calculate the rate of heat transfer. A schematic of the apparatus is shown in Figure 1 and a photograph is shown in Figure 2. Using a needle valve to control the flow rate, compressed air (Praxair - 99.9% purity) was flowed into the a stainless steel tubing over a length of 300 mm towards the nanoparticle injection system. The air flow rate and pressure were monitored using an OMEGA FMA-1612 flow meter and Ashcroft pressure gauge, respectively.

Preconditioned nanoparticles were dispersed into the flow through a custom-built injection system. An off-balance electric motor provided constant frequency oscillations to a particle reservoir, which controlled the flow rate of the gravity-fed particles through a 0.75 mm diameter orifice. Figure 3 shows a scanning electronic microscope (SEM) image of the particles. The Al2O3 particles are approximately spherical with mean diameter of 90-120 nm. Although individual particle size remained consistent, agglomerates and aggregates size varied from 5-50 um. The thermophysical properties of Al2O3 particles are as follows: density = 3970 kg/m^3; specific heat = 880 J/kgK; thermal conductivity = 30 W/mK.[42]

After injection, the particles and air mixed over a tube length of 508 mm before reaching the hot-wire assembly. The hot-wire consisted of a 1 mm diameter Nichrome wire. It was housed in a custom-built machinable ceramic tube (inner diameter of 10.16 mm) and sealed using Resbond 907GF high temperature (1288°C) sealing putty. Sorensen DCR40-20A power supply was used to provide current to the hot-wire through a 14-gage insulated wire. For the heat transfer calculations, temperature of the hot-wire was calculated from resistance measurements and was maintained between 500-700 °C. A 1Ω shunt resistor was used to accurately calculate current passing through the Nichrome wire. Voltage readings were recorded

using an NI USB-6363 DAQ and LabVIEW^{TM} 2012 software. Data acquisition took place over a period of 30 seconds at a sample rate of 1 kHz. Due to fluctuations in the particle flow injection rate, data was averaged over a duration of 30 seconds.

Two NTC thermistors, Thermistor PN 103JL1A from U.S. Sensor, were used to monitor and record the temperature of the mixture upstream and downstream of hot-wire. Resistance of each thermistor was indirectly measured by recording voltage drop and current. Current was calculated based on voltage drop across a 10KΩ shunt resistor. Heat loss from the stainless steel tubing to the surrounding air in the laboratory was minimized by applying 12.7 mm thick foam insulation. 240 mm downstream of the final thermistor, the nanoaerosol was decelerated in a 753 mm^3 collection tank. Particles were collected inside the tank using a borosilicate glass microfibres bonded with Kynar fluorocarbon resin filter. The filter was obtained from Headline Filters and rated at 95+% filtration of 0.1 micron particles and aerosols. After running for approximately 30 seconds, air flow and particle injection was stopped and the collection tank was disconnected from the apparatus and weighed using a HR-AZ analytical balance. The mass of particles accumulated in the collection tank in combination with the time duration of the experiment was used to determine the particle mass flow rate. The air and particle mass flow rates were used to calculate the particle mass loading, S_L. After each experiment the system was flushed with compressed air at 20-30 psig for 2 minutes to remove residual particles.

A set of air-only tests were conducted to provide a baseline and to assess the accuracy and repeatability of the apparatus, the results of which are discussed below. The Reynolds number, based on the mean air flow velocity and the tubing diameter, was varied from 1,420 to 10,310. Note that the Reynolds number based on the hot-wire diameter varied from 142-1031. In this work, the Reynolds number based on the tubing diameter is reported. At three Reynolds number dwells (6,000, 7,500, and 8,900), particle injection tests were performed using various particle mass loadings (0.01%-0.1%). The global Nusselt number was calculated from the measured temperature rise of the mixture, the effective mixture properties based on the particle mass loading, and the local flow conditions. Note that each test condition (including air-only tests) was performed in a random fashion to minimize bias error and demonstrate repeatability.

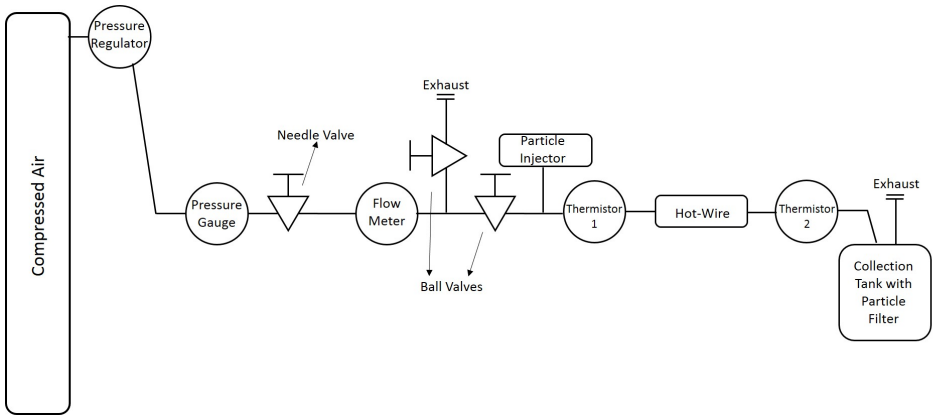

Figure 1. Schematic of experimental set-up.

III. Results

A. Mixture Properties

Physical and thermophysical properties of Al_2O_3-air nanoaerosol were estimated from analytical models reported in the literature.[27] Note that these models have mainly been applied to Al_2O_3-water nanofluids but should still be applicable to gas-based nanofluids. The effective density is calculated from:

$$\rho_{eff} = \frac{m_f + m_p}{V_f + V_p} = \frac{\rho_f V_f + \rho_p V_p}{V_f + V_p} = (1 - \Phi_p)\rho_f + \Phi_p \rho_p \tag{1}$$

where Φ_p refers to the volume fraction of the particles. The effective heat capacity is calculated assuming thermal equilibrium between the nanoparticles and the base fluid:

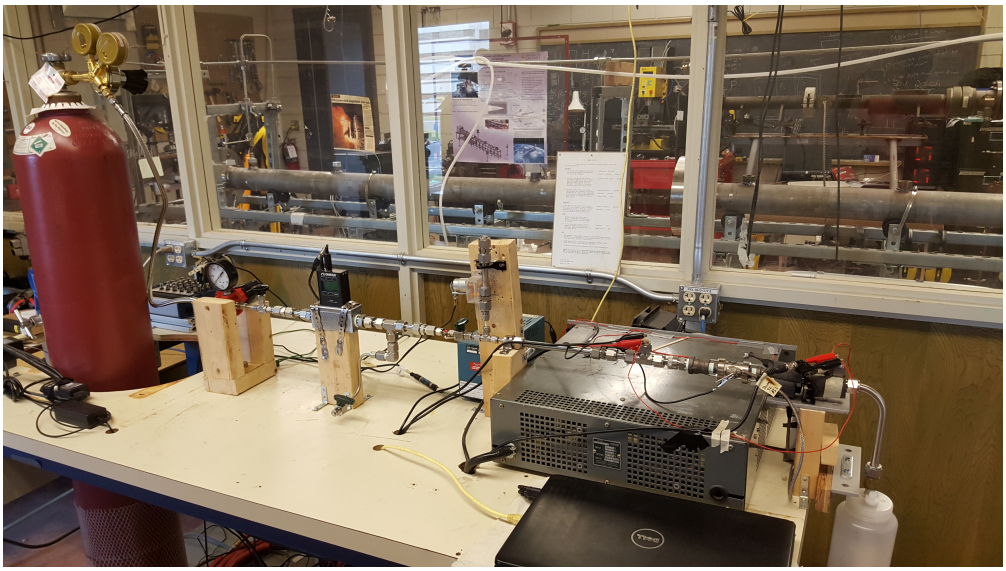

Figure 2. Photo of experimental set-up.

$$c_{eff} = \frac{(1-\Phi_p)\rho_f c_f + \Phi_p \rho_p c_p}{\rho_{eff}} \tag{2}$$

Brinkmans model for two-phase mixtures was used to estimate the effective dynamic viscosity. The model is valid for particle volume fractions less than 2%.[27]

$$\mu_{eff} = \frac{\mu_f}{(1-\Phi_p)^{2.5}} \tag{3}$$

The effective thermal conductivity was estimated using Hamilton-Crosser model:

$$k_{eff} = \frac{k_p + (n-1)k_f + (n-1)\Phi_p(k_p - k_f)}{k_p + (n-1)k_f - \Phi_p(k_p - k_f)} k_f \tag{4}$$

The model is appropriate for low volume fractions ($\Phi_p \leq 4\%$) and for thermal conductivity ratios greater than 100 ($k_p/k_f \geq 100$). The model is also sensitive to the shape of the particles, which is represented by empirical shape factor, n. For spherical particles, n=3, whereas for cylindrical particles, n=6. As evident from Figure 3, Al2O3 particles are approximately spherical (n≈3). Note that the Hamilton-Crosser model assumes that the thermal conductivity is independent of particle size and particle temperature.

The mixture Reynolds number was calculated using the effective density and effective dynamic viscosity. Similarly, the Prandtl number was calculated using models for effective heat capacity and effective thermal conductivity. Properties of the base fluid (air) and Al2O3 particles were obtained from Incropera (2011).[42]

$$Re_D = \frac{\rho_{eff} U D}{\mu_{eff}} \tag{5}$$

$$Pr = \frac{c_{eff}\mu_{eff}}{k_{eff}} \tag{6}$$

B. Air-Only Tests

Air-only experiments are performed over a Reynolds number range of 1500-11,200. The Nusselt number is calculated based on the static temperature rise of the gas measured downstream of the hot-wire. Assuming steady state, the overall heat transfer coefficient is calculated by equating the rate of heat transfer to the change in enthalpy of the gas:

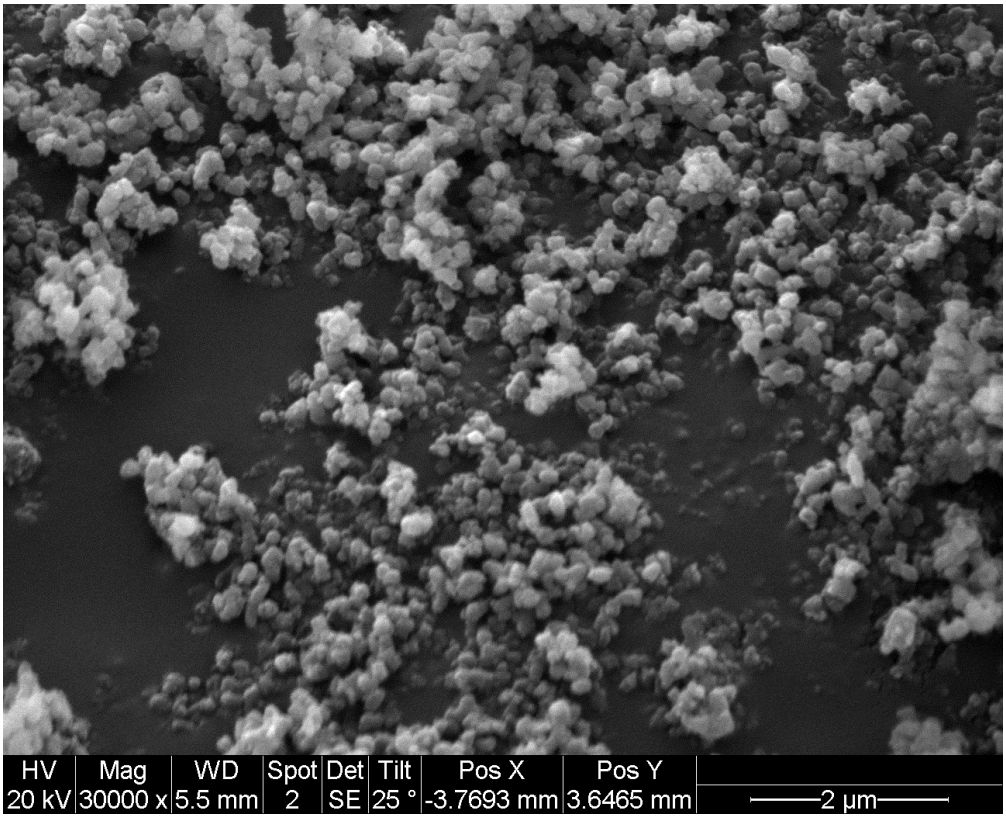

Figure 3. SEM image of Al2O3 particles

$$Q = mC_p(T_d - T_u) = hA(T_s - T_u) \tag{7}$$

where T_d, T_u, and T_s are temperature downstream of hot-wire, temperature upstream of hot-wire, and temperature at the surface of hot-wire,respectively. Once the convective heat transfer coefficient is known, the Nusselt number can be computed using hot-wire diameter, D_w, from the following equation:

$$Nu = \frac{hD_w}{k} \tag{8}$$

Figure 4 shows a comparison of experimental Nusselt number values and the Nusselt number computed from the empirical relation of Zukauskas:[42]

$$Nu_D = ARe_D^b Pr^x (\frac{Pr}{Pr_s})^{\frac{1}{4}} \tag{9}$$

where

A=0.51, b=0.5 for $40 \geq \mathrm{Re_D} \leq 1000$
A=0.26, b=0.6 for $1001 \geq \mathrm{Re_D} \leq 200000$

The Zukauskas relation has an uncertainty of 20%.[42] Good agreement is demonstrated at the higher Reynolds numbers. Discrepancies at the lower Reynolds number are attributed to a likely transitional flow regime, heat losses to pipe walls, and lower signal-to-noise levels of the measurement equipment.

C. Particle Tests

Experiments with particles were performed at Reynolds numbers of 6000, 7500, and 8900, which correspond to air flow rates of 45, 55 and 65 SLPM, respectively. The choice to fix the Reynolds number while varying

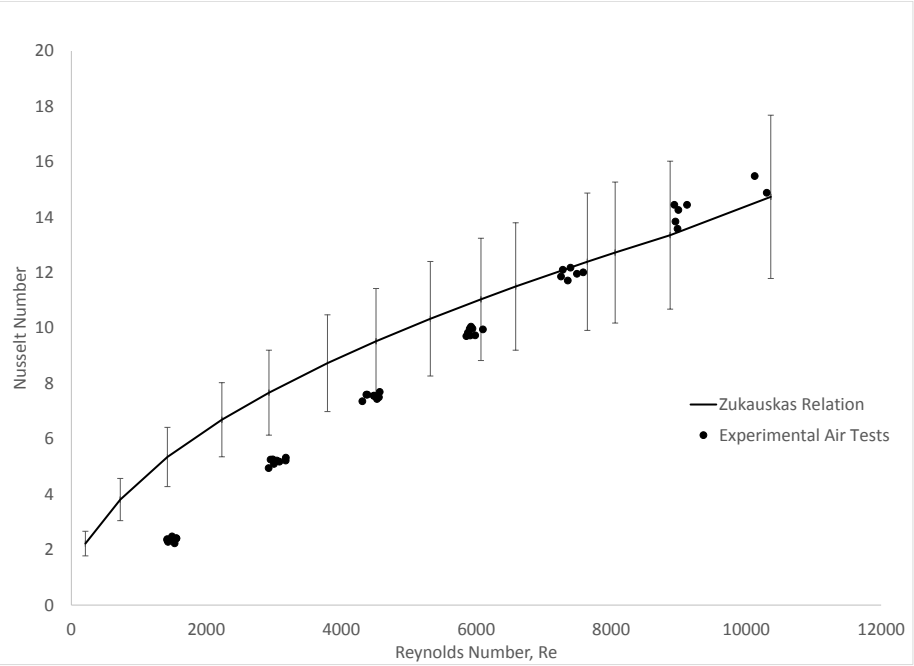

Figure 4. Validation of experimental setup

the particle mass loading was largely governed by challenges associated with controlling the particle injection rate. The inability to precisely control the particle loading rate was compensated by the ability to accurately measure the particle flow rate after each experiment was completed. At each Reynolds number, approximately 10 tests with varying particle mass loadings were performed. Experimental Nusselt numbers were computed using the same methodology described for the air-only tests, but were based on mixture thermophysical properties shown in Equations 1-4.

Figures 5-7 show the effect of mass loading on Nusselt number at each Reynolds number. It is clear that the increase in Nusselt number is positively correlated to the particle mass loading. Power-law curve fits were applied to each Reynolds number condition and the R^2 values are reported in each figure. Since the particle mass loading could not be precisely controlled, the power-law fits in Figures 5-7 were used to determine the effect of particle mass loading over a range of Reynolds numbers (Figure 9). The error bars shown in the figure correspond to one standard deviation of the experimental data.

IV. Discussion

The results indicate that only a small particle mass loading (<0.1%) is required to provide a large increase to the global Nusselt number (50%). While the observed trend of increasing heat transfer enhancement with increasing particle mass loading is consistent with theory reported in the literature,[39] there are few experiments to compare against. Murray performed similar cross-flow heat transfer experiments with 58 micron diameter glass beads and found that a particle mass loading of approximately 100% was required to produce 50% increase in Nusselt number. However, the particles used in the current work are approximately 580 times smaller in diameter and the Reynolds number based on the wire diameter in the current work is approximately 13 times lower than what was reported by Murray. Murray's results show an exponential increase in Nusselt number enhancement with decreasing particle size and a linear increase in Nusselt number

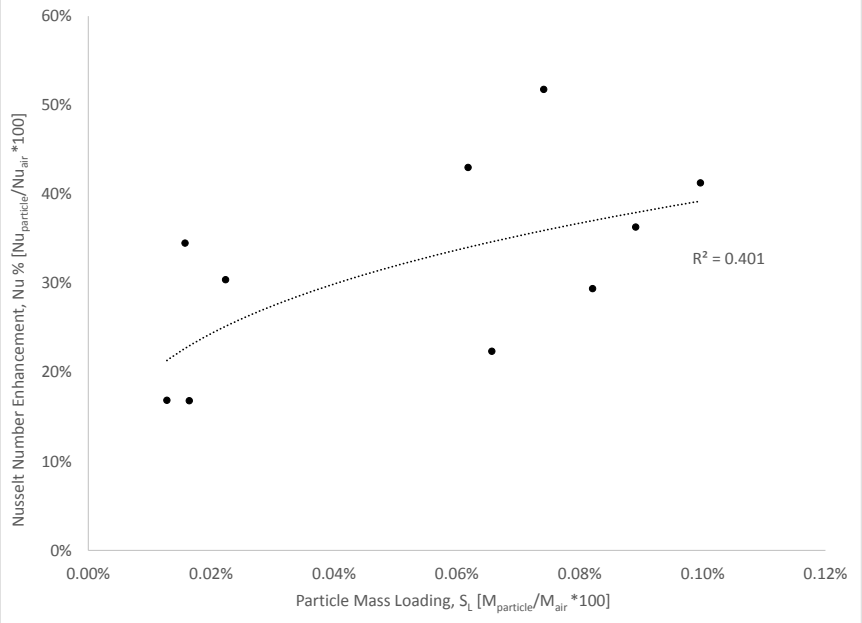

Figure 5. Effect of mass loading on Nusselt number ratio at Re = 6000

enhancement with decreasing Reynolds number. It is possible that the combination of smaller particle size, lower Reynolds number, and lower particle loading balance to give similar levels of heat transfer enhancement for the two cases.

Additional work needs to be performed to further understand the results. Murray's heat transfer models should be implemented to predict expected levels of heat transfer enhancement at these test conditions. The magnitude of additional heat transfer mechanisms, such as thermophoresis, Brownian diffusion or radiative heat transfer between particles, which are assumed to be negligible, need to be analyzed. Additional tests at each Reynolds number need to be performed to improve the quality of the data set. Experiments with larger diameter particles and different material types need to be performed.

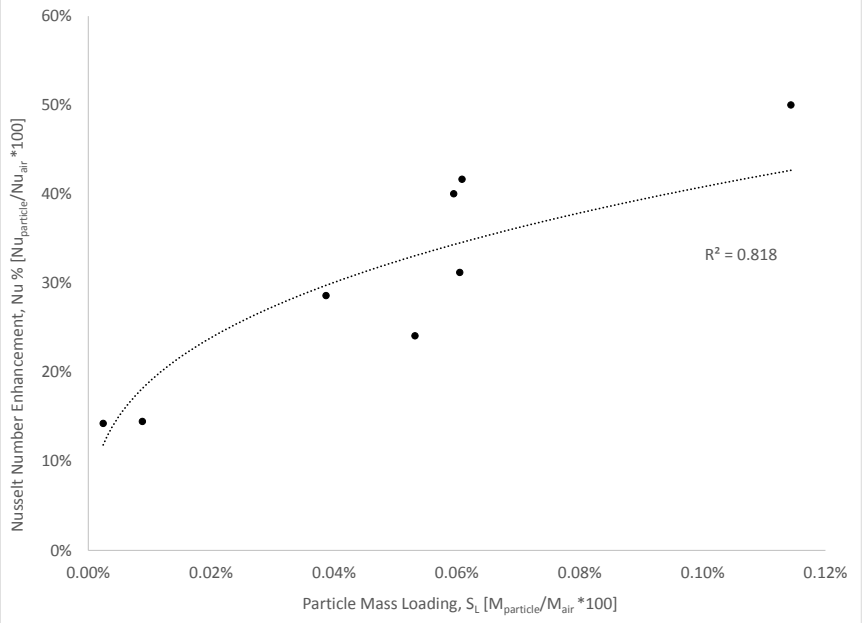

Figure 6. Effect of mass loading on Nusselt number ratio at Re = 7500

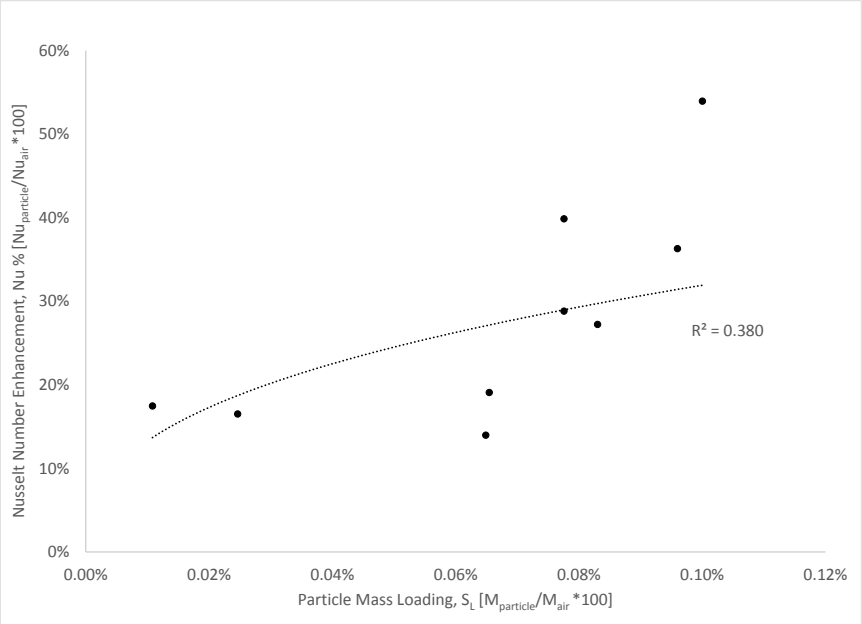

Figure 7. Effect of mass loading on Nusselt number ratio at Re = 8900

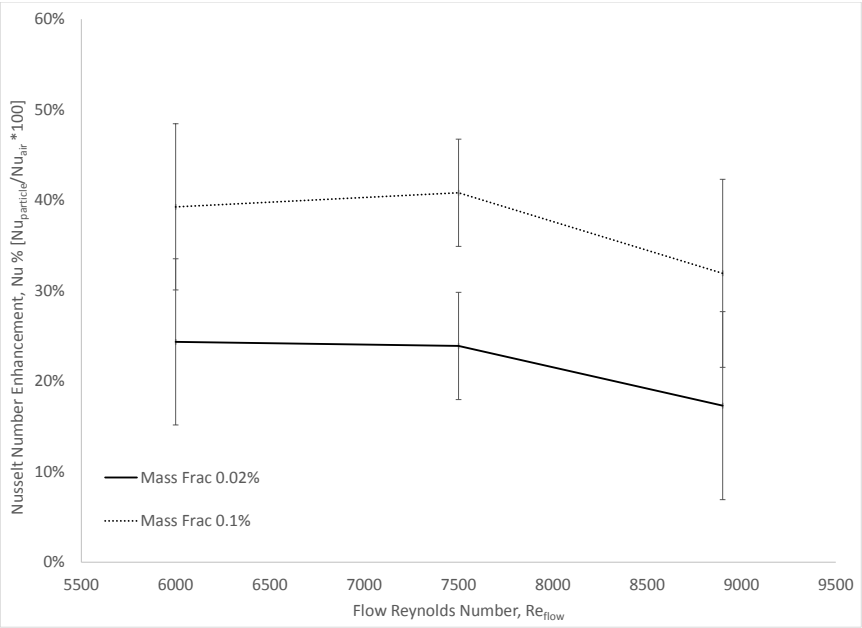

Figure 8. Variance in Nusselt number ratio due to Reynolds number

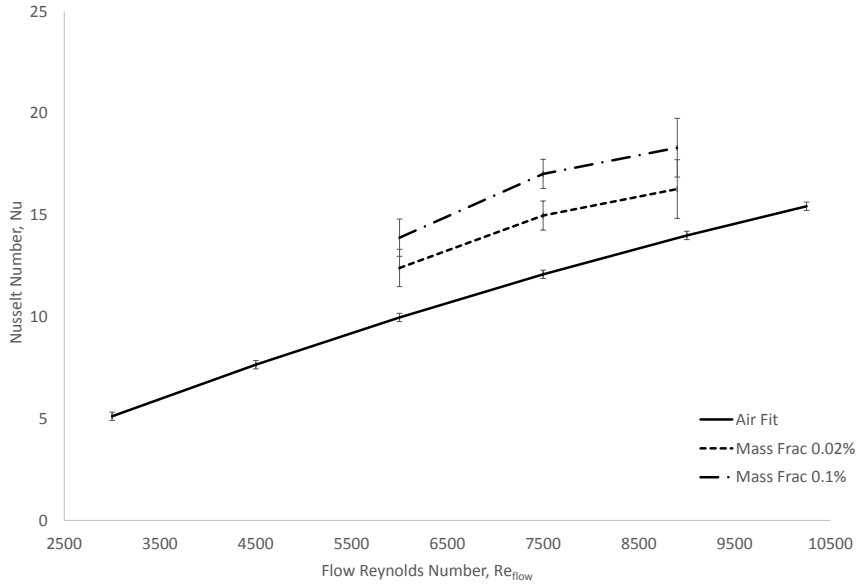

Figure 9. Effect of particle mass loading on Nusselt number at various Reynolds numbers

V. Conclusion

The enhancement of convective heat transfer due to the suspension of nano-Al_2O_3 particles in air has been demonstrated experimentally. The experimental apparatus was validated through a comparison of air-only test results to established empirical relations of convective heat transfer for a cylinder in cross-flow. A large magnitude of heat transfer enhancement (15%-50%) was observed for relatively low particle mass loadings (0.01%-0.1%) between Reynolds number range of 6000-8900. The observed trends are consistent with theory proposed by Murray but the enhancements are much larger than magnitudes observed in similar micron-sized heat transfer experiments. Differences in particle diameter and Reynolds number are proposed to explain the discrepancy. The results are still considered to be preliminary and more experimental testing and analysis is required.

VI. Acknowledgments

The authors would like to acknowledge the financial support of Space Engine Systems Inc., through the Natural Sciences and Engineering Research Council (NSERC) of Canada's Collaborative Research Development (CRD) grant. The authors would also like to acknowledge financial support from Alberta Innovates Technology Futures (AITF) through Dr. Johansen's Strategic Chair position (iCORE).

References

[1]Choi, S. U. S., "Enhancing themal conductivity of fluids with nanoparticles," *ASME-Publications*, Vol. 231, 1995, pp. 99–106.

[2]Minkowycz, W., Sparrow, E., and Abraham, J., *Nanoparticle Heat Transfer and Fluid Flow*, Vol. 20124236, 2012.

[3]Das, S. K., Choi, S. U. S., and Patel, H. E., "Heat Transfer in NanofluidsA Review," *Heat Transfer Engineering*, Vol. 27, No. 10, 2006, pp. 3–19.

[4]Schluderberg, D., Whitelaw, R., and Carlson, R., "Gaseous suspensions - A new reactor coolant," *Nucleonics*, Vol. 19, No. 8, 1961.

[5]Goroshin, S., Higgins, A., and Kamel, M., "Powdered Metals as Fuel for Hypersonic Ramjets," *37th AIAA/ASME/SAE/ASEE Joint Propulsion Conference and Exhibit*, 2001.

[6]Huang, Y., Risha, G. a., Yang, V., and Yetter, R. a., "Effect of particle size on combustion of aluminum particle dust in air," *Combustion and Flame*, Vol. 156, No. 1, 2009, pp. 5–13.

[7]Murthy, S. and Curran, E., "High-Speed Propulsion Systems," *AIAA Progress in Astronautics and Aeronautics Series*, Vol. 137, 1991.

[8]Varvill, R. and Bond, A., "A comparison of propulsion concepts for SSTO reusable launchers," *JBIS - Journal of the British Interplanetary Society*, Vol. 56, No. 3-4, 2003, pp. 108–117.

[9]Jivraj, F., Varvill, R., Bond, A., and Paniagua, G., "The Scimitar Precooled Mach 5 Engine," *2nd European conference for aerospace sciences (EUCASS)*, 2007, pp. 1–10.

[10]Choi, S. U. S., "Nanofluids: From Vision to Reality Through Research," *Journal of Heat Transfer*, Vol. 131, No. March 2009, 2009, pp. 033106.

[11]Wong, K. V. and De Leon, O., "Applications of nanofluids: Current and future," *Advances in Mechanical Engineering*, Vol. 2010, 2010.

[12]Bianco, V., Chiacchio, F., Manca, O., and Nardini, S., "Numerical investigation of nanofluids forced convection in circular tubes," *Applied Thermal Engineering*, Vol. 29, No. 17-18, 2009, pp. 3632–3642.

[13]Shafahi, M., Bianco, V., Vafai, K., and Manca, O., "An investigation of the thermal performance of cylindrical heat pipes using nanofluids," *International Journal of Heat and Mass Transfer*, Vol. 53, No. 1-3, 2010, pp. 376–383.

[14]Shafahi, M., Bianco, V., Vafai, K., and Manca, O., "Thermal performance of flat-shaped heat pipes using nanofluids," *International Journal of Heat and Mass Transfer*, Vol. 53, No. 7-8, 2010, pp. 1438–1445.

[15]Khanafer, K., Vafai, K., and Lightstone, M., "Buoyancy-driven heat transfer enhancement in a two-dimensional enclosure utilizing nanofluids," *International Journal of Heat and Mass Transfer*, Vol. 46, 2003, pp. 3639–3653.

[16]Khaled, a. R. a. and Vafai, K., "Heat transfer enhancement through control of thermal dispersion effects," *International Journal of Heat and Mass Transfer*, Vol. 48, 2005, pp. 2172–2185.

[17]Eastman, J. a., Choi, S. U. S., Li, S., Yu, W., and Thompson, L. J., "Anomalously increased effective thermal conductivities of ethylene glycol-based nanofluids containing copper nanoparticles," *Applied Physics Letters*, Vol. 78, No. 2001, 2001, pp. 718–720.

[18]Jang, S. P. and Choi, S. U. S., "Role of Brownian motion in the enhanced thermal conductivity of nanofluids," *Applied Physics Letters*, Vol. 84, No. 2004, 2004, pp. 4316–4318.

[19]Lee, S. and Choi, S. U., "Application of metallic nanoparticle suspensions in advanced cooling systems," *Engineering Conference*, 1997.

[20]Ali, a., Vafai, K., and Khaled, a. R. a., "Comparative study between parallel and counter flow configurations between air and falling desiccant in the presence of nanoparticle suspensions," *International Journal of Energy Research*, Vol. 27, No. October 2002, 2003, pp. 725–745.

[21]Putra, N., Roetzel, W., and Das, S. K., "Natural convection of nano-fluids," *Heat and Mass Transfer/Waerme- und Stoffuebertragung*, Vol. 39, 2003, pp. 775–784.

[22]Xuan, Y. and Li, Q., "Heat transfer enhancement of nanofluids," *International Journal of Heat and Fluid Flow*, Vol. 21, 2000, pp. 58–64.

[23]Xuan, Y. and Li, Q., "Investigation on Convective Heat Transfer and Flow Features of Nanofluids," *Journal of Heat Transfer*, Vol. 125, No. February 2003, 2003, pp. 151.

[24]Pak, B. C. and Cho, Y. I., "Hydrodynamic and Heat Transfer Study of Dispersed Fluids With Submicron Metallic Oxide Particles," *Experimental Heat Transfer*, Vol. 11, No. January 2015, 1998, pp. 151–170.

[25]Ho, C. J., Liu, W. K., Chang, Y. S., and Lin, C. C., "Natural convection heat transfer of alumina-water nanofluid in vertical square enclosures: An experimental study," *International Journal of Thermal Sciences*, Vol. 49, 2010, pp. 1345–1353.

[26]Zhou, S.-Q. and Ni, R., "Measurement of the specific heat capacity of water-based Al2O3 nanofluid," *Applied Physics Letters*, Vol. 92, No. 2008, 2008, pp. 093123.

[27]Khanafer, K. and Vafai, K., "A critical synthesis of thermophysical characteristics of nanofluids," *International Journal of Heat and Mass Transfer*, Vol. 54, No. 19-20, 2011, pp. 4410–4428.

[28]El Bécaye Maïga, S., Palm, S. J., Nguyen, C. T., Roy, G., and Galanis, N., "Heat transfer enhancement by using nanofluids in forced convection flows," *International Journal of Heat and Fluid Flow*, Vol. 26, 2005, pp. 530–546.

[29]Buongiorno, J., "Convective Transport in Nanofluids," *Journal of Heat Transfer*, Vol. 128, No. March 2006, 2006, pp. 240.

[30]Nguyen, C. T., Desgranges, F., Roy, G., Galanis, N., Maré, T., Boucher, S., and Angue Mintsa, H., "Temperature and particle-size dependent viscosity data for water-based nanofluids - Hysteresis phenomenon," *International Journal of Heat and Fluid Flow*, Vol. 28, 2007, pp. 1492–1506.

[31]Hamilton, R. . L. and Crosser, O. K., "Thermal Conductivity of Hetrogenous Two-Component Systems," *I & EC Fundamentals*, Vol. 1, No. 3, 1959, pp. 187–191.

[32]Kakaç, S. and Pramuanjaroenkij, A., "Review of convective heat transfer enhancement with nanofluids," *International Journal of Heat and Mass Transfer*, Vol. 52, No. 13-14, 2009, pp. 3187–3196.

[33]Heris, S. Z., Etemad, S. G., and Esfahany, M. N., "Experimental investigation of oxide nanofluids laminar flow convective heat transfer," *International Communications in Heat and Mass Transfer*, Vol. 33, 2006, pp. 529–535.

[34]Wen, D. and Ding, Y., "Experimental investigation into the pool boiling heat transfer of aqueous based gamma-alumina nanofluids," *Journal of Nanoparticle Research*, Vol. 7, 2005, pp. 265–274.

[35]Wang, B. X., Zhou, L. P., and Peng, X. F., "A fractal model for predicting the effective thermal conductivity of liquid with suspension of nanoparticles," *International Journal of Heat and Mass Transfer*, Vol. 46, 2003, pp. 2665–2672.

[36]Das, S. K., Putra, N., Thiesen, P., and Roetzel, W., "Temperature Dependence of Thermal Conductivity Enhancement for Nanofluids," *Journal of Heat Transfer*, Vol. 125, No. August 2003, 2003, pp. 567.

[37]Das, S. K., Putra, N., and Roetzel, W., "Pool boiling of nano-fluids on horizontal narrow tubes," *International Journal of Multiphase Flow*, Vol. 29, 2003, pp. 1237–1247.

[38]Das, S. K., Putra, N., and Roetzel, W., "Pool boiling characteristics of nano-fluids," *International Journal of Heat and Mass Transfer*, Vol. 46, 2003, pp. 851–862.

[39]Murray, D. B., "Local enhancement of heat transfer in a particulate cross flow - I Heat transfer mechanisms," *International Journal of Multiphase Flow*, Vol. 20, No. 3, 1994, pp. 493–504.

[40]Bianco, V., Manca, O., Nardini, S., and Vafai, K., *Heat Transfer Enhancement With Nanofluids*, No. April, CRC Press, 2015.

[41]Murray, D., "Local enhancement of heat transfer in a particulate cross flowII Experimental data and predicted trends," *International Journal of Multiphase Flow*, Vol. 20, No. 3, 1994, pp. 505–513.

[42]Incropera, F. P., DeWitt, D. P., Bergman, T. L., and Lavine, A. S., *Fundamentals of Heat and Mass Transfer*, Vol. 6th, 2007.